Radiation Dose–Volume Effects on Negative Tumor-Draining Lymph Nodes Affected T-cell Activation and Prognosis in Esophageal Cancer with Chemoradiotherapy

Ihsuan Tseng[1,2,3,4,5,6], Yun Chen[1,2,3,4], Dashan Ai[1,2,3,4], Zhengfei Zhu[1,2,3,4], Weixin Zhao[1,2,3,4], Min Fan[1,2,3,4], Ling Li[1,2,3,4], Hongcheng Zhu[1,2,3,4], Fangfang Li[7], Yang Xu[8], Lu Yu[9], Zezhou Wang[2,10,11], Juanqi Wang[1], Qi Liu[1,2,3,4], Jiaying Deng[1,2,3,4], Shengnan Hao[1,2,3,4], Qingsong Fan[12], Jinjun Ye[13], Jialiang Zhou[14], Chaoyang Wu[15], Huarong Tang[16], Qin Lin[17], Jiancheng Li[18], Yunhai Li[19], Shihong Wei[20], Hui Luo[21], Jianzhong Cao[22], Xiangpeng Zheng[23], Guang Huang[24], Yuwei Zheng[2,25,26], Bo Ping[2,25,26], and Kuaile Zhao[1,2,3,4]

ABSTRACT

Purpose: A preclinical model found that elective nodal irradiation attenuated the efficacy of radiotherapy (RT) and radioimmunotherapy. However, limited clinical studies have explored the correlation between radiation dose–volume parameters of negative tumor-draining lymph nodes (TDLN) and T-cell activation/prognosis for patients with cancer treated with definitive radiochemotherapy.

Experimental Design: Patients with locally advanced esophageal cancer undergoing definitive chemoradiotherapy (CRT) were selected from two prospective trials. Dose–volume parameters of TDLN as well as other lymphocyte-related organs at risk and lymphocyte subsets such as $CD3^{-}CD19^{+}$ B cells, $CD8^{+}CD28^{+}$ T cells, and activated T cells ($CD3^{+}CD8^{+}HLA\text{-}DR^{+}$) before and at the end of RT were collected. Logistic analysis was utilized to correlate dose–volume parameters with reductions in lymphocyte subsets. Prognosis of TDLN irradiation was investigated through Kaplan–Meier analysis and Cox hazards models.

Results: Among 512 patients, the median mean dose of TDLN and negative non-TDLN was 25.6 and 15.1 Gy, respectively. Multivariable analyses indicated that TDLN V15 >50% was an independent predictor of poorer local recurrence–free survival (HR, 1.31; $P = 0.029$) and distant metastasis–free survival (HR, 1.39; $P < 0.001$), as well as greater reductions in $CD3^{-}CD19^{+}$ B cells (OR, 1.98; $P = 0.002$), $CD8^{+}CD28^{+}$ T cells (OR, 3.42; $P < 0.001$), and $CD3^{+}CD8^{+}HLA\text{-}DR^{+}$ T cells (OR, 4.67; $P = 0.002$) after RT.

Conclusions: A higher radiation dose–volume parameter of TDLNs in patients with esophageal cancer undergoing CRT was significantly associated with suppression of T-cell activation and a worse prognosis. Limiting the percentage of TDLN V15 may be beneficial for improving the prognosis of CRT with or without PD-1 inhibitors.

Introduction

The activation of antitumor immunity is increasingly recognized as a critical determinant of the overall clinical effectiveness of radiotherapy (RT) on both targeted and distant tumors (1). A cornerstone in this understanding is the ability of RT to induce immunogenic death of tumor cells, promoting the release of tumor antigens and subsequent T-cell activation. Supporting this notion, preclinical studies have underscored the importance of an intact immune system in combating radioresistance and inhibiting metastatic spread after RT, as evidenced

[1]Department of Radiation Oncology, Fudan University Shanghai Cancer Center, Shanghai, China. [2]Department of Oncology, Shanghai Medical College, Fudan University, Shanghai, China. [3]Shanghai Clinical Research Center for Radiation Oncology, Shanghai, China. [4]Shanghai Key Laboratory of Radiation Oncology, Shanghai, China. [5]Department of Radiation Oncology, Shanghai Proton and Heavy Ion Center, Shanghai, China. [6]Shanghai Key Laboratory of Radiation Oncology, Shanghai Engineering Research Center of Proton and Heavy Ion Radiation Therapy, Shanghai, China. [7]Center for Cancer Immunology, Institute of Biomedicine and Biotechnology, Shenzhen Institutes of Advanced Technology, Chinese Academy of Sciences, Shenzhen, China. [8]Department of Medicine, Enhance Human Health Through Pharma Technology Innovation, Shanghai, China. [9]Shanghai Medical College of Fudan University, Shanghai, China. [10]Department of Cancer Prevention, Fudan University Shanghai Cancer Center, Shanghai, China. [11]Shanghai Municipal Hospital Oncological Specialist Alliance, Shanghai, China. [12]Department of General Practice, Changhai Community Healthcare Center, Shanghai, China. [13]Department of Radiation Oncology, Jiangsu Cancer Hospital, Nanjing, China. [14]Department of Radiation Oncology, Affiliated Hospital of Jiangnan University, Wuxi, China. [15]Department of Radiation Oncology, Zhenjiang First People's Hospital, Zhenjiang, China. [16]Department of Radiation Oncology, Zhejiang Cancer Hospital, Hangzhou, China. [17]Department of Radiation Oncology, The First Affiliated Hospital of Xiamen University, Xiamen, China. [18]Department of Radiation Oncology, Fujian Provincial Cancer Hospital, Fuzhou, China. [19]Department of Radiation Oncology, Minhang Branch Hospital, Fudan University Shanghai Cancer Center, Shanghai, China. [20]Department of Radiation Oncology, Gansu Cancer Hospital, Lanzhou, China. [21]Department of Radiation Oncology, Jiangxi Cancer Hospital, Nanchang, China. [22]Department of Radiation Oncology, Shanxi Cancer Hospital, Taiyuan, China. [23]Department of Radiation Oncology, Huadong Hospital Affiliated to Fudan University, Shanghai, China. [24]Department of Radiation Oncology, Hainan People's Hospital, Haikou, China. [25]Department of Pathology, Fudan University Shanghai Cancer Center, Shanghai, China. [26]Institute of Pathology, Fudan University, Shanghai, China.

Corresponding Author: Kuaile Zhao, Department of Radiation Oncology, Fudan University Shanghai Cancer Center, 270 DongAn Road, Shanghai 200032, China. E-mail: kuaile_z@fudan.edu.cn

Clin Cancer Res 2025;31:2024–33

doi: 10.1158/1078-0432.CCR-24-4123

Translational Relevance

Some clinical trials on locoregional cancers have revealed unexpected results that concurrently adding an anti–PD-1/PD-L1 antibody to chemoradiotherapy (CRT) did not improve overall survival compared with CRT alone, contradicting preclinical findings. Although animal studies demonstrated that elective nodal irradiation attenuated the efficacy of radio-immunotherapy, few clinical investigations have addressed this issue. This study is the first to characterize negative lymph node regions and explore their correlation with T-cell activation and prognosis. It found that a higher dose volume of lymph node irradiation was associated with diminished T-cell activation and poorer prognosis. These results offer a potential explanation for negative outcomes in certain clinical trials and suggest that lymph node irradiation may serve as a valuable parameter for evaluating T-cell activation and prognosis for locoregional cancer treated with immunotherapy and CRT.

by increased radiation doses required for similar tumor control effects in immunocompromised mice (2).

Central to this immune response is the tumor-draining lymph node (TDLN), acting as a critical site for priming T-cell activation and facilitating the generation of radiation-induced cytotoxic T cells. The capture, transport, processing, and presentation of peripheral antigens in the lymph nodes are mediated by specialized antigen-presenting cells (APC), which culminate in the activation of tumor antigen–specific T cells for cancer cell elimination (3). Experimental findings from TDLN-deficient mice and mice with TDLNs surgically ablated have shown impaired tumor control (radioresistance) and limited "abscopal effect" (metastasis) following RT (4, 5). T-cell activation hinges on dual signals. The first signal comes from antigen recognition by the T-cell receptor binding to MHCs on APCs. The second signal is delivered when CD28 on the T-cell surface is engaged by B7 molecules on the same APC (2). Moreover, B cells, which constitute 40% in lymph nodes (6), not only serve as APCs (7) but also bolster the cytotoxic functions of tumor-specific $CD8^+$ T cells, in collaboration with effective $CD4^+$ T follicular helper cells (8).

Although elective nodal irradiation (ENI) continues to be a common practice in specific cancer treatments, recent preclinical studies suggest that ENI may compromise the effectiveness of RT and radio-immunotherapy. The immunologic effects of TDLN irradiation may include reduced peripheral blood lymphocytes (9), impaired antigen presentation and activation of T cells in lymph nodes (9–11), and a decrease in tumor microenvironment (TME) chemokines leading to a decline in cytotoxic T cells (10). Recent clinical trials for locoregional lung cancer (12), nasopharyngeal cancer (13), head and neck cancer (14, 15), and cervical cancer (16) revealed surprising results that the addition of an anti–PD-1/PD-L1 antibody to chemoradiotherapy (CRT) did not improve overall survival (OS; ref. 14), contrary to findings from preclinical studies (1). The authors supposed that ENI-induced immunosuppression might account for the limited efficacy of combining CRT with immunotherapy.

The TDLN, being a radiosensitive lymphocyte-rich organ, plays a pivotal role in immune responses. Establishing a nuanced understanding of the relationship between TDLN irradiation and systemic immunity/prognosis is imperative for advancing TDLN-sparing RT technology, which aims to safeguard overall immunity and optimize the efficacy of RT and immunotherapy. However, studies addressing this issue from a clinical perspective are scarce. Building on this gap in research, our study aimed to investigate the potential impacts of TDLN irradiation on prognosis and circulating antitumor immunity in patients with esophageal cancer receiving definitive concurrent CRT (dCCRT) through a re-analysis of clinical data from two prospective clinical trials.

Materials and Methods

Patient selection

This longitudinal study was performed in compliance with the Declaration of Helsinki (1975) and was based upon two prospective randomized clinical trials: ESO-Shanghai 1 (17) and ESO-Shanghai 2 (18), which were approved by the Ethics Committee of Fudan University Shanghai Cancer Center (1203108-4 and 1505146-13), and written informed consent was provided by all patients before sampling.

All patients were diagnosed with locally advanced esophageal squamous cell carcinoma (ESCC) and received dCCRT. This study included four chemotherapy regimens: fluorouracil with cisplatin; fluorouracil with paclitaxel (PTX); PTX with cisplatin; and PTX with carboplatin. The planning RT regimen was 1.8 Gy/fraction, 5 days/week, to a total dose of 61.2 Gy, using involved field irradiation based on intensity-modulated RT with six MV photons. The gross tumor volume (GTV) comprised the esophageal tumor and metastatic lymph nodes, which were diagnosed based on at least one of the following criteria: (i) pathologic confirmation and (ii) a short axis of ≥10 mm in the mediastinum or cervix or ≥5 mm in the tracheoesophageal groove. The clinical target volume was defined as the GTV expanded manually by 3 cm only in the superior–inferior direction for the primary tumor, with no expansion for metastatic lymph nodes. The planning target volume (PTV) represented a further 1 cm expansion from the clinical target volume in all directions. Detailed information on the treatment regimen and dose–volume constraints of important organs at risk (OAR) could be found in previous protocols (ClinicalTrials.gov identifier: NCT01591135 and NCT02459457). The exclusion criteria for this study were as follows: (i) actual received dose <50.4 Gy; (ii) no course of chemotherapy completed; (iii) absence of absolute lymphocyte count (ALC) during RT or lymphocyte subsets at baseline or the end of RT; (iv) no qualified-plan images available for re-delineation; and (v) RT suspended ≥1 month. The screening strategy for this study was displayed in Supplementary Fig. S1. Clinical features such as gender, age, tumor location, tumor length, tumor stage, etc., were collected for analysis (17, 18).

Collection and analyses of lymphocytes and subsets by flow cytometry

Fresh venous blood samples were collected for blood routine and flow cytometry testing at baseline (within 8 weeks before RT) and at the end of RT (within 2 weeks before and 4 weeks after the end of RT). Total lymphocytes and subsets including $CD3^+$, $CD3^+CD4^+$, $CD3^+CD8^+$, regulatory T cells (Treg) ($CD4^+CD25^+CD127^{low/-}$), $CD8^+CD28^+$ T cells, $CD3^-CD(16+56)^+$ NK cells, $CD3^-CD19^+$ B cells, and activated $CD8^+$ T cells ($CD3^+CD8^+HLA\text{-}DR^+$) were collected. Specific and isotype-matched monoclonal antibodies were used for detection, including CD3 (PE, APC, and FITC conjugated; RRID: AB_400287, AB_400513, and AB_400405), CD4 (FITC

conjugated, RRID: AB_3674897), CD8 (FITC conjugated, RRID: AB_399998), CD16 + CD56 (PE conjugated, RRID: AB_2868707), CD25 (APC conjugated, RRID: AB_400551), CD127 (PE conjugated, RRID: AB_131301), CD45 (PerCP-CY5.5 conjugated), CD28 (PE conjugated, RRID: AB_399998), CD19 (APC conjugated, RRID: AB_400510), and HLA-DR (PerCP-CY5.5 conjugated, RRID: AB 10718537; Supplementary Fig. S2). Fluorescent markers were determined by BD FACSCanto I and quantified on Diva software.

ALC data from baseline including weekly during CRT until the end of RT were obtained and graded according to the Common Terminology Criteria for Adverse Events version 5.0. The lymphocyte nadir was defined as the lowest ALC value appearing during CRT, and its grade was denoted as G.

The absolute count of a particular type of lymphocyte subset was the total lymphocyte count from blood routine multiplied by the differential percentage of that cell type. The residual ratio (RR) of a lymphocyte subset was defined as the value of its absolute count at the end of RT divided by that before RT.

$$\text{Residual ratio (RR)} = \frac{\text{absolute counts at the end of RT}}{\text{absolute counts before RT}}$$

Delineations of lymphocyte-related organs at risk

Negative lymph nodes were defined as all lymph node regions within the scanning field excluding GTV, from the cricothyroid membrane to the abdominal trunk layer. These negative lymph node regions were further categorized into TDLNs, following the American Joint Committee on Cancer (AJCC) 8th edition for esophageal cancer, which included supraclavicular regions, stations 2, 4, 7 to 9, and 15 to 20, whereas the remaining areas were classified as negative non-TDLNs (TDLNs and non-TDLNs mentioned in this study both referred to negative lymph nodes). Delineation principles were guided by a cross-sectional nodal atlas organized by Monge, and colleagues (19). The diagram of lymph node delineation of a patient is displayed in Supplementary Fig. S3.

The bone marrow, spleen, body, heart, and lungs within the scanned regions were delineated by threshold-based segmentation and manual correction (13). The dose–volume values of lymphocyte-related OARs (LOARs), denoted as Vx, which are defined as the percentage of a total organ volume receiving no less than x Gy of radiation, were obtained from dose–volume histograms (DVH). The mean doses of the body, heart, and lungs were collected to calculate the effective dose to immune cells developed by Jin and colleagues (20).

Statistical analysis

Measurement data (such as age, tumor length, etc.) were expressed as median and IQR. Principal component analysis was used to summarize the largest source of variation from DVHs (Supplementary Fig. S4), by which principal components were proved to have similar effects with traditional dose–volume parameters (21). Data of lymphocyte subsets were classified into two groups by their corresponding medians: >the median and ≤the median. The Vx (V5, V10, V15, V20, V25, V30, and V45) of TDLN (non-TDLN Vx would be consistent with it) and its optimal cutoff were determined by the result, with the lowest P value using maximally selected log-rank statistics (MaxStat analysis) based on OS. Logistic analysis was performed to explore the relationships between TDLN Vx and changes of lymphocytes. The predictive values were estimated by AUCs from the ROC curve and were compared by the Delong test. Kaplan–Meier analysis was used to compare the differences in survival outcomes between groups, and the Cox hazards model was used to estimate HRs with their 95% confidence intervals (CI). Variables with $P < 0.05$ on univariate analysis were entered into multivariable analysis. A two-tailed $P < 0.05$ was considered to be significant. All analyses were performed using R studio version 4.2.1 (RRID: SCR 001905) and Graphpad Prism 9.0 software (RRID: SCR 002798).

Data availability

The data supporting the findings of this study are available within the article and its supplementary materials. Other datasets generated and analyzed during this study are not publicly available because of ethical restrictions and patient privacy concerns. However, reasonable requests for access to de-identified data may be directed to the corresponding author.

Results

The characteristics of clinical features, lymphocytes, and dose–volume parameters

A total of 512 patients (78.5% males and 21.5% females) were eligible, with a median age of 63 years (IQR, 57–69 years). Among them, 139 (27.1%), 243 (47.5%), and 130 (25.4%) patients were diagnosed with stage II, III, and IV (referring to TxNxM1a and TxNxM1b based on lymph node status, rather than the presence of metastases in other organs according to the American Joint Committee on Cancer 6th edition), respectively. The majority of the tumors were located in the cervical or upper esophagus ($n = 297$, 58%), with a median tumor length of 6.0 cm (IQR, 4.0–7.0 cm). A total of 432 patients (84.4%) completed 61.2 Gy RT. Fifty-nine percent of patients received monthly concurrent chemotherapy (fluorouracil with cisplatin or PTX with cisplatin) and 41% weekly (fluorouracil with PTX or PTX with carboplatin).

Data of total lymphocytes and subsets were collected in 512 patients. The median baseline ALC was 1.57×10^9/L (IQR, 1.30–2.02×10^9/L) and the count declined to 0.87, 0.72, 0.58, 0.48, 0.39, 0.42, and 0.42×10^9/L from weeks 1 to 7, respectively. The cumulative incidence of G0 to G3 and G4 ALC nadir during RT was 60.9% and 39.1%, respectively. The absolute counts of lymphocyte subsets, such as $CD3^+CD8^+$ (24.76×10^7/L vs. 11.10×10^7/L), $CD3^-CD19^+$ B cells (15.73×10^7/L vs. 0.94×10^7/L), and $CD8^+CD28^+$ T cells (8.81×10^7/L vs. 2.35×10^7/L), were significantly decreased at the end of RT. Among these subsets, $CD3^-CD19^+$ cells exhibited the greatest decrease with a median RR of 0.06. Activated $CD8^+$ T cells were tested successfully in 133 patients. The absolute counts of $CD3^+CD8^+HLA\text{-}DR^+$ T cells before and at the end of RT were 4.66×10^7/L (IQR, 2.52–8.26×10^7/L) and 3.28×10^7/L (IQR, 1.16–8.68×10^7/L). The RR of activated $CD8^+$ T cells was 0.63 (IQR, 0.22–1.48). Visualization of treatment-induced changes in immune cell subsets could be found in Supplementary Fig. S5.

Dosimetric parameters of 512 patients were successfully collected. The median mean dose of TDLN and non-TDLN was 25.6 and 15.1 Gy. The median values of TDLN V5, V15, V30, and V45 were 48.3%, 45.0%, 44.0%, and 37.5%, respectively, and those of non-TDLN were 53.4%, 33.5%, 19.7%, and 11.1%, respectively.

Other details in clinical features, lymphocytes, and dose–volume parameters are shown in **Table 1** and Supplementary Table S1.

The impact of TDLN irradiation on prognosis

The median follow-up for all patients was 59.6 months. Of 512 patients available for survival analysis, 272 (53.1%) patients died during

Table 1. The characteristics of clinical features, lymphocytes, and dose–volume parameters.

Characteristic	Data (*N* = 512)	Characteristic	Data (*N* = 512)
Clinical features		**Lymphocytes**	
Age, years	63 (57–69)[a]	ALC	
Sex, no. (%)		Baseline ALC, 10^9/L	1.57 (1.30–2.02)[a]
Male	402 (78.5)	G4 ALC nadir, no. (%)	200 (39.1)
Female	110 (21.5)	G0 to G3 ALC nadir, no. (%)	312 (60.9)
ECOG score, no. (%)		**T cells**	
0	366 (71.5)	$CD3^+$	
1–2	146 (28.5)	Baseline of RT, 10^7/L	103.11 (82.30–133.92)[a]
Clinical stage, no. (%)		The end of RT, 10^7/L	32.78 (21.55–46.52)[a]
II	139 (27.1)	RR	0.31 (0.21–0.45)
III	243 (47.5)	$CD3^+CD4^+$	
IV[b]	130 (25.4)	Baseline of RT, 10^7/L	37.57 (27.07–50.77)[a]
Location, no. (%)		The end of RT, 10^7/L	10.11 (6.20–16.05)[a]
Cervical + upper	297 (58.0)	RR	0.28 (0.17–0.41)
Middle + lower	200 (39.1)	$CD3^+CD8^+$	
Multiple	15 (2.9)	Baseline of RT, 10^7/L	24.76 (16.24–37.30)[a]
Tumor length, cm	6.0 (4.0–7.0)[a]	The end of RT, 10^7/L	11.10 (5.70–18.07)[a]
RT dose, no. (%)		RR	0.43 (0.24–0.72)
61.2 Gy	432 (84.4)	$CD4^+CD25^+CD127^{low/-}$ (Treg)	
50.4 ~ < 61.2 Gy	80 (15.6)	Baseline of RT, 10^7/L	3.81 (2.49–5.59)[a]
Chemotherapy regimen, no. (%)		The end of RT, 10^7/L	1.13 (0.61–13.83)[a]
Monthly (PF + TP)	302 (59.0)	RR	0.30 (0.16–0.52)
Weekly (TF + TC)	210 (41.0)	$CD8^+CD28^+$	
		Baseline of RT, 10^7/L	8.81 (5.60–13.58)[a]
Dose–volume parameters		The end of RT, 10^7/L	2.35 (1.18–4.45)[a]
GTV, cm^3	40.8 (24.5–69.2)[a]	RR	0.27 (0.16–0.45)
EDIC, Gy	7.4 (5.3–10.3)[a]	$CD3^+CD8^+HLA\text{-}DR^+$ (N = 133)	
TDLN		Baseline of RT, 10^7/L	4.66 (2.52–8.26)[a]
Size, cm^3	249.6 (181.6–331.3)[a]	The end of RT, 10^7/L	3.28 (1.16–8.68)[a]
Mean dose, Gy	25.6 (21.7–31.3)[a]	RR	0.63 (0.22–1.48)[a]
non-TDLN		**Other subsets**	
Size, cm^3	376.9 (303.2–469.8)[a]	$CD3^-CD16^+ \pm CD56^+$	
Mean dose, Gy	15.1 (11.8–18.7)[a]	Baseline of RT, 10^7/L	34.62 (23.59–50.07)[a]
Spleen		The end of RT, 10^7/L	8.05 (4.75–13.83)[a]
Size, cm^3	117.0 (69.9–168.0)[a]	RR	0.25 (0.15–0.41)[a]
Mean dose, Gy	32.9 (21.3–56.7)[a]	$CD3^-CD19^+$	
Bone marrow		Baseline of RT, 10^7/L	15.73 (10.15–22.47)[a]
Size, cm^3	1779.1 (1,538.0–1984.1)[a]	The end of RT, 10^7/L	0.94 (0.51–1.61)[a]
Mean dose, Gy	12.0 (10.0–14.0)[a]	RR	0.06 (0.03–0.10)[a]

Abbreviations: ECOG, Eastern Cooperative Oncology Group; EDIC, effective dose to immune cells; PF, fluorouracil with cisplatin; TC, PTX with carboplatin; TF, fluorouracil with PTX; TP, PTX with cisplatin.

[a]Data expressed as median with IQR.

[b]Stage IV here was classified as TxNxM1a and TxNxM1b based on lymph node status, rather than the presence of metastases in other organs according to American Joint Committee on Cancer 6th edition (patients with TxNxM1a had cervical lymph node metastasis in upper ESCC or abdominal lymph node metastasis in lower ESCC, whereas TxNxM1b referred to supraclavicular lymph node metastasis).

the follow-up period with a median OS of 49.1 months. Among these patients, 5-year local recurrence–free survival (LRFS) and 5-year distant metastasis–free survival (DMFS) was 45.1% and 44.7%, respectively, with a corresponding median time of 39.5 and 37.7 months.

Based on the result of MaxStat analysis, the V15 was chosen and the optimal cutoff was 50% for TDLN V15 and 40% for non-TDLN V15 (Supplementary Fig. S6). The Kaplan–Meier curves and univariable Cox analyses (Supplementary Table S2) demonstrated that patients with TDLN V15 > 50% had poorer OS (**Fig. 1A**; $P < 0.001$), LRFS (5-year LRFS, 35.6% vs. 50.1%; $P < 0.001$; **Fig. 1B**), and DMFS (5-year DMFS, 33.9% vs. 50.4%; $P < 0.001$; **Fig. 1C**). Moreover, non-TDLN V15 > 40% also possibly tended toward poorer clinical outcomes (**Fig. 1D–F**).

Multivariable analysis in **Table 2** further revealed TDLN V15 > 50% to be an independent prognostic factor for poorer OS (HR, 1.41; 95% CI, 1.09–1.83; $P = 0.010$), LRFS (HR, 1.31; 95% CI, 1.03–1.66; $P = 0.029$), and DMFS (HR, 1.38; 95% CI, 1.08–1.77; $P = 0.011$), whereas non-TDLN V15 > 40% failed to demonstrate prognostic value in multivariable analysis (**Fig. 1D–F**).

Among 105 of 512 (20.5%) patients without lymph node metastasis (TxN0M0), 19 patients with TDLNV15 >50% demonstrated poorer clinical outcomes (Breslow $P < 0.05$, Supplementary Fig. S7A–S7C). On the other side, in the remaining 407 patients with lymph node metastasis, 158 patients with TDLN V15 >50% were also more likely to have poorer clinical outcomes (log-rank $P < 0.05$, Supplementary Fig. S7D–S7F).

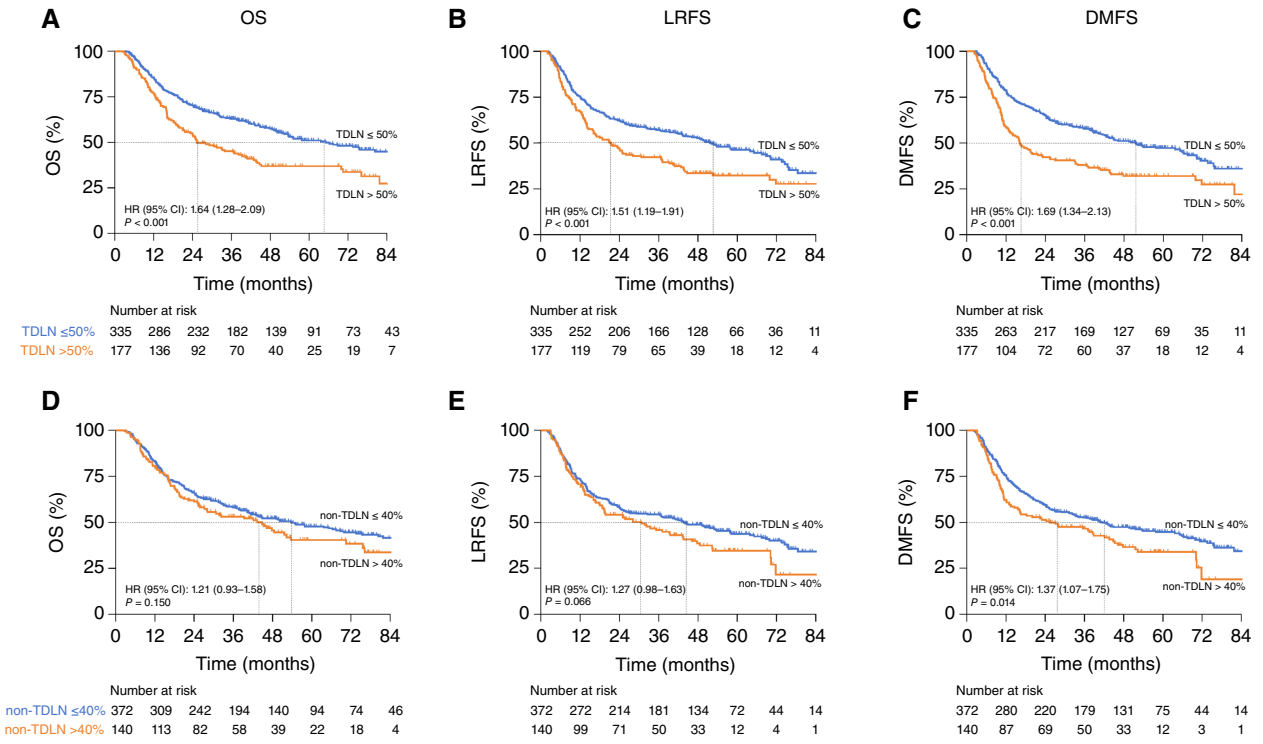

Figure 1.
Survival outcomes for patients with TDLN V15 >50% vs. ≤50% (**A–C**), and non-TDLN V15 >40% vs. ≤40% (**D–F**).

The effect of TDLN irradiation on T-cell activation

Univariable analyses indicated a potential association between TDLN V15 > 50% and lower RRs across various lymphocyte subsets (Supplementary Table S3). Subsequent multivariable analysis (Supplementary Table S4) confirmed a significant link between TDLN V15 >50% and lower RRs of $CD3^+$ T cells (OR, 3.05; 95% CI, 2.01–4.61; $P < 0.001$). Upon dividing T cells into $CD4^+$ (OR, 2.39; 95% CI, 1.54–3.71; $P < 0.001$) and $CD8^+$ T cells (OR, 1.98; 95% CI, 1.36–2.88; $P < 0.001$), adjusted results consistently demonstrated higher TDLN V15 associated with lower RRs. Additionally in **Table 3**, a lower RR of $CD19^+$ B cells was correlated with higher TDLN V15 (OR, 1.98; 95% CI, 1.28–3.05; $P = 0.002$), which was also influenced by spleen irradiation ($P < 0.001$). A lower RR of $CD8^+CD28^+$ T cells was both influenced by higher TDLN V15 (OR, 3.42; 95% CI, 2.20–5.31; $P < 0.001$) and non-TDLN V15 (OR, 1.69; 95% CI, 1.07–2.68; $P = 0.026$). Notably, TDLN V15 > 50% was found to be more pertinent to a lower RR of $CD3^+CD8^+$HLA-DR^+ T cells (OR, 4.67; 95% CI, 1.80–12.01; $P = 0.002$). Furthermore, multivariable adjustments incorporating other TDLN Vx parameters or V15 as a continuous variable (Supplementary Tables S5 and S6) consistently demonstrated significant correlations between TDLN irradiation and changes in $CD3^-CD19^+$, $CD8^+CD28^+$, and $CD3^+CD8^+$HLA-DR^+ cells.

Building upon previous findings of a poor prognostic trend in G4 ALC nadir during RT (Supplementary Fig. S8; Supplementary Table S7), multivariable results in Supplementary Tables S8 and S9 also exhibited a TDLN V15 >50% significant predictive value for severe lymphopenia (OR, 5.21; 95% CI, 3.28–8.28; $P < 0.001$).

Fig. 2A–D intuitively displayed the distributions of AUCs concerning dose–volume parameters of LOARs that predict lower RRs of $CD19^+$, $CD8^+CD28^+$, and $CD3^+CD8^+$HLA-DR^+ cells, as well as G4 ALC nadir. Comparisons in the DVHs of TDLN versus non-TDLN among groups are shown in **Fig. 3A–D**.

The impact of lymphocyte subsets on prognosis

Using the optimal cutoff values determined by MaxStat for the RRs of each lymphocyte subset, Kaplan–Meier analyses preliminarily revealed that lymphocyte subsets, except for $CD3^+$ and activated $CD8^+$ T cells (data not shown), were significantly correlated with survival outcomes ($P < 0.05$; Supplementary Fig. S9A–S9F).

Discussion

This study represents the first attempt to delineate TDLNs and non-TDLNs and to analyze the DVH parameters of these lymph nodes. The results unveiled that patients receiving higher dose–volume parameters of TDLNs, as opposed to non-TDLNs and other LOARs, exhibited lower RRs of lymphocyte subsets associated with T-cell activation and poorer prognosis.

Lymph nodes are rich in lymphocytes. Most lymphocytes do not remain in the peripheral blood for a long time but rather migrate from the blood to the lymphatic tissue and then back to the blood. A study measuring chromosomal aberrations of breast cancer with RT revealed that the quantity of lymph nodes within the radiation field significantly influenced

Table 2. Multivariate Cox analysis of TDLN irradiation for survival outcomes.

	OS		LRFS		DMFS	
Characteristic	**HR (95% CI)**	***P***	**HR (95% CI)**	***P***	**HR (95% CI)**	***P***
Age		**0.017**		**0.012**		0.054
>63 years	0.75 (0.59–0.95)		0.75 (0.59–0.94)		0.80 (0.64–1.00)	
≤63 years	Ref		Ref		Ref	
Sex		**0.024**		**0.011**		**0.019**
Male	1.48 (1.05–2.08)		1.53 (1.10–2.11)		1.48 (1.07–2.05)	
Female	Ref		Ref		Ref	
Clinical stage		**0.048**		**0.016**		**0.016**
II	0.73 (0.54–0.99)		0.69 (0.51–0.94)		0.69 (0.51–0.93)	
III + IV[a]	Ref		Ref		Ref	
Location	—	—	—	—		0.120
Cervical + upper					0.83 (0.65–1.05)	
Middle + lower + multiple					Ref	
GTV, cm^3	1.01 (1.00–1.01)	<**0.001**	1.01 (1.00–1.01)	<**0.001**	1.00 (1.00–1.01)	**0.002**
TDLN V15		**0.005**		**0.029**		**0.010**
>50%	1.43 (1.11–1.83)		1.31 (1.03–1.66)		1.39 (1.08–1.78)	
≤50%	Ref		Ref		Ref	
non-TDLN V15	—	—	—	—		0.191
>40%					1.19 (0.92–1.53)	
≤40%					Ref	

Variables with $P < 0.05$ on univariate were entered into multivariate. A "—" in the table indicates that this factor failed to show statistical significance in the univariable analysis. *P* values < 0.05 are in bold.

Abbreviation: Ref, reference.

[a]Stage IV here was classified as TxNxM1a and TxNxM1b based on lymph node status, rather than the presence of metastases in other organs according to American Joint Committee on Cancer 6th edition (patients with TxNxM1a had cervical lymph node metastasis in upper ESCC or abdominal lymph node metastasis in lower ESCC, whereas TxNxM1b referred to supraclavicular lymph node metastasis).

the occurrence of RT-induced chromosomal aberrations in peripheral blood lymphocytes (22, 23). Our study emphasized the crucial role of TDLN in severe RT-induced lymphopenia, compared with other LOARs. This may be attributed to (i) lymphocyte proliferation that occurs mainly in lymph nodes, which renders them more susceptible to radiation sensitivity than other organs; (ii) lymphocytes being mobile cells that continuously circulate between blood and tissues via the lymphatic system, with a re-circulation time of about 20 to 30 hours, aligning with the 24-hour interfraction interval in conventional RT (24); and (iii) TDLNs, located nearer to the GTV being likely to receive higher radiation doses, as another study found that an expanded PTV corresponded to increased irradiation of lymph nodes, with PTV identified as a contributing factor in G4 lymphopenia (25).

Another pivotal discovery was that irradiating TDLNs, rather than non-TDLNs, significantly suppressed systemic immunity, leading to decreased $CD8^+CD28^+$ T and B cells and poorer prognosis. Lymph nodes house approximately 60% of T cells and 40% of B cells, creating an optimal environment for CTL activation (3). TDLNs are primary sites for tumor antigen presentation associated with lymphocyte activation. The release of damage-associated molecular pattern molecules from dying and stressed cells following RT/chemotherapy triggers Toll-like receptor (TLR9) engagement on innate-like B cells (refs. 26, 27) or APCs (7) within the TME. The activation and proliferation of B and T cells enhance their capacity for efficient antigen presentation and the activation of adaptive immunity. Irradiating these activated cells in the TDLNs can hinder T-cell activation. Based on established statistical standards, the percent of the TDLN volume exceeding 15 Gy (V15) was a promising parameter for predicting the risk of systemic immunosuppression. A total dose of 15 Gy, about 0.5 Gy per fraction, was delivered to the TDLN, aligning with lymphocyte radiosensitivity, as *in vitro* studies showed average α values of B cells, T cells, and NK cells at ~0.4 Gy-1, ~0.3 Gy-1, and ~0.3 Gy-1, respectively, with a dose as low as 0.5 Gy inducing significant lymphocyte death (28). Improving the accuracy of lymph node metastasis diagnosis, reducing elective irradiation of normal lymph nodes, and limiting the percentage of TDLN V15 may help reduce systemic immunosuppression and improve the prognosis of CRT.

Preclinical studies demonstrated that combining PD-1 inhibitors with radiation enhanced therapeutic efficacy (1, 10), and a prospective clinical study observed systemic $CD8^+$ T-cell activation after adding metastasis-directed RT to systemic therapy, which correlated with improved PFS and OS in oligometastatic pancreatic ductal adenocarcinoma (29). However, concurrent additional PD-1 inhibitor to about 30 daily dCCRT did not significantly improve OS compared with dCCRT alone for locally advanced cancer, such as lung cancer (12), nasopharyngeal cancer (13), head and neck cancer (14, 15), and cervical cancer (16) in randomized clinical trials, which some authors attributed to immunosuppression from ENI used with PD-1 inhibitors, although in unresectable locally advanced ESCC, many clinical trials are still ongoing to determine the efficacy of combining immunotherapy and CRT (30). Both mouse models and human studies identified that TDLNs played a role in modulating antitumor responses to immunotherapy.

Table 3. Multivariate logistic analysis for lower RRs of lymphocyte subsets.

	$CD3^-CD19^+$		$CD8^+CD28^+$		[a]$CD3^+CD8^+HLA\text{-}DR^+$	
	≤0.06 vs. >0.06		**≤0.27 vs. >0.27**		**≤0.63 vs. >0.63**	
Characteristic	**OR (95% CI)**	***P***	**OR (95% CI)**	***P***	**OR (95% CI)**	***P***
Age	—	—	—	—		0.104
>63 years					0.49 (0.21–1.16)	
≤63 years					Ref	
Sex		0.114	—	—		**0.007**
Male	1.47 (0.91–2.38)				4.39 (1.50–12.78)	
Female	Ref				Ref	
Clinical stage		0.073	—	—	—	—
II	0.63 (0.38–1.05)					
III + IV[b]	Ref					
Location		**0.016**	—	—	—	—
Cervical + upper	0.55 (0.34–0.89)					
Middle + lower + multiple	Ref					
Tumor length		0.417	—	—	—	—
>6 cm	0.83 (0.54–1.30)					
≤6 cm	Ref					
Chemotherapy regimen	—	—		**0.017**	—	—
Monthly (PF + TP)			0.63 (0.43–0.92)			
Weekly (TF + TC)			Ref			
GTV, cm^3	1.01 (1.00–1.01)	0.069	1.01 (1.00–1.01)	0.063	1.00 (0.99–1.01)	0.623
TDLN V15		**0.002**		**<0.001**		**0.002**
>50%	1.98 (1.28–3.05)		3.42 (2.20–5.31)		4.67 (1.80–12.01)	
≤50%	Ref		Ref		Ref	
non-TDLN V15		0.686		**0.026**	—	—
>40%	1.10 (0.69–1.77)		1.69 (1.07–2.68)			
≤40%	Ref		Ref			
Marrow[c]	1.00 (1.00–1.01)	0.235	1.00 (1.00–1.01)	0.174	—	—
Spleen[c]	1.01 (1.00–1.01)	**<0.001**	1.00 (1.00-1.00)	0.227	1.00 (1.00–1.01)	0.885
EDIC, Gy	0.95 (0.87–1.04)	0.243	—	—	—	—

Variables with $P < 0.05$ on univariate were entered into multivariate. A "—" in the table indicated that this factor failed to show statistical significance in the univariable analysis. *P* values < 0.05 are in bold.

Abbreviations: EDIC, effective dose to immune cells; PF, fluorouracil with cisplatin; TC, PTX with carboplatin; TF, fluorouracil with PTX; TP, PTX with cisplatin.

[a]The logistic analysis of activated $CD8^+$ T cells was calculated in the population of 133 patients.

[b]Stage IV here was classified as TxNxM1a and TxNxM1b based on lymph node status, rather than the presence of metastases in other organs according to American Joint Committee on Cancer 6th edition (patients with TxNxM1a had cervical lymph node metastasis in upper ESCC or abdominal lymph node metastasis in lower ESCC, whereas TxNxM1b referred to supraclavicular lymph node metastasis). The RR of a lymphocyte subset was the value of the absolute counts at the end of RT divided by that at baseline.

[c]The spleen-related/bone marrow–related dose–volume parameter included in this analysis was represented by the principal component 1 of spleen/bone marrow DVH.

Removing TDLNs during anti–PD-1 therapy almost abrogated the tumor-suppressive effects of the treatment (31, 32). Recently, substantial benefits were observed in early-stage non–small cell lung cancer treated with immunotherapy combined with stereotactic ablative RT, likely because of stereotactic ablative RT dosing or its role in minimizing lymphopenia by targeting smaller volumes and sparing lymph nodes from irradiation (33). Our study showed that the patients with TDLN V15 > 50% had greater reductions in B cells, $CD28^+$ T cells, active $CD8^+$ T cells, and poorer OS in ESCC treated with dCCRT. Both GTV and TDLN V15 were significantly associated with survival outcomes in univariable analysis. Although TDLN V15 was partially influenced by GTV ($r = 0.33$; $P < 0.001$), multivariate analysis still confirmed TDLN as an independent prognostic factor. These findings suggest that constraining TDLN V15 may be crucial for improving the efficacy of PD-1 inhibitors combined with CRT.

With regard to the correlations between lymphocyte subsets and prognosis, we considered that the rough classification of $CD3^+$ T cells and the small population of activated $CD8^+$ T cells might be attributed to the negative findings. Although we prioritized the role of TDLN in this article and did not delve deeply into this issue, the observed associations between multiple subsets and prognosis highlighted the complexity of their effects on outcomes. These findings emphasize the necessity for more precise subset classification and further investigation in preclinical studies to elucidate their underlying mechanisms.

Nevertheless, our study has several limitations: (i) the ambiguity in defining TDLN and non-TDLN in esophageal cancer presents challenges; (ii) markers related to antigenic presentation, T-cell activation, and cytotoxic effects were not detected; (iii) the absence of pathologic examination of tumors and lymph nodes after RT impedes our understanding of the impact of TDLN irradiation on the TME and lymph nodes; (iv) 18 patients

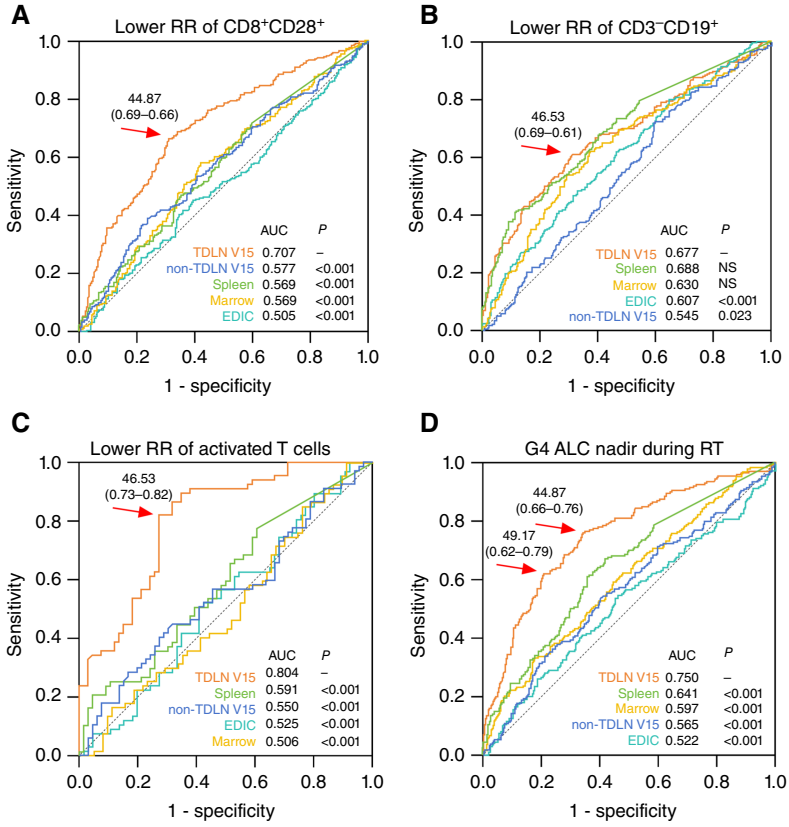

Figure 2.

A–D, ROCs of LOARs predicting lower RRs of lymphocyte subsets and G4 ALC nadir during RT. The AUC values and corresponding *P* values compared with that of TDLN V15 were recorded in the bottom right corner. The Youden index with corresponding sensitivity and specificity was marked in each figure. The RR of a lymphocyte subset was the value of the absolute counts at the end of RT divided by that at baseline. The spleen-related/bone marrow–related dose–volume parameter included in this analysis was represented by the principal component 1 of spleen/bone marrow DVH. The analysis of activated $CD8^+$ T cells was calculated in the population of 133 patients.

(3.5%) had final blood results 2 to 4 weeks after completing CCRT, potentially affecting the reliability of the results; and (v) although different chemotherapy regimens did not affect the RT dose, their cytotoxic effects were varied. In all, it remains to be confirmed whether this TDLN RT parameter truly affects the efficacy of RT combined with PD-1 inhibitors.

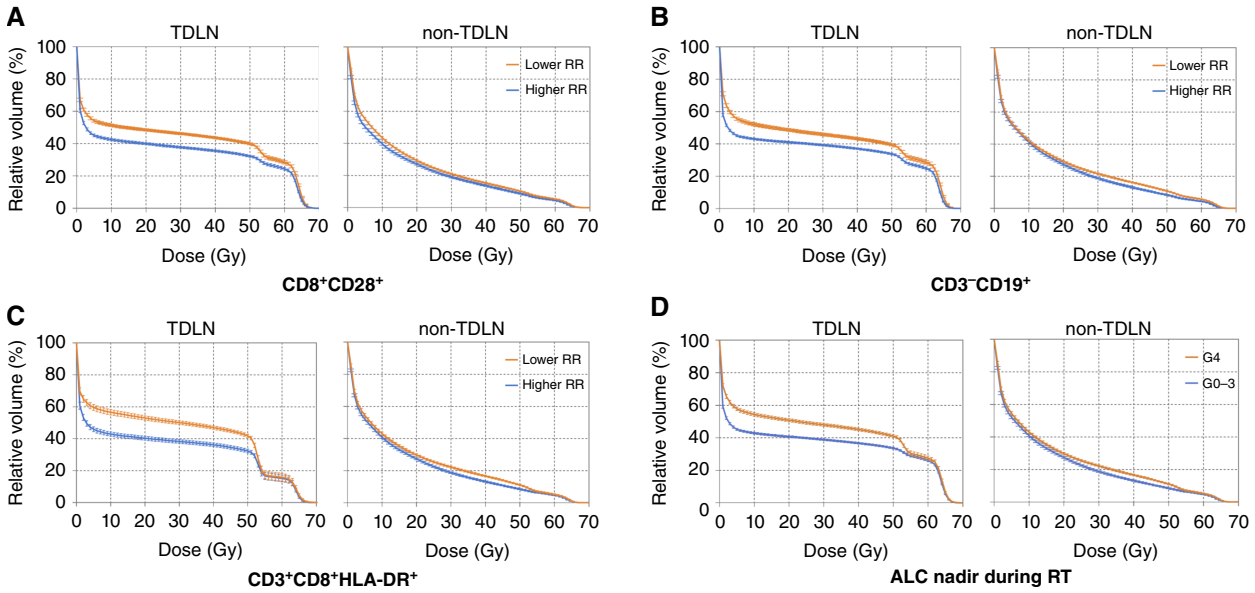

Figure 3.

A–D, The DVHs of TDLN and non-TDLN between groups. The solid line was connected by the mean values of each point in patients and the error bar presented the SE of the mean. The RR of a lymphocyte subset was the value of the absolute counts at the end of RT divided by that at baseline.

Conclusions

This study is the first to reveal that higher radiation exposure to TDLNs of patients undergoing CRT produces a pronounced decrease in $CD8^+CD28^+$ T cells and $CD3^-CD19^+$ B cells, indicating a dampening of activated T-cell response. The patients with a TDLN V15 >50% showed immunosuppression and poor prognosis. To further validate TDLN V15 as a parameter for assessing T-cell activation and prognosis for locoregional cancer treated with a combination of immunotherapy and CRT, we are conducting a prospective randomized clinical trial (ESO-Shanghai 26, NCT 06676449).

Authors' Disclosures

No disclosures were reported.

Authors' Contributions

I. Tseng: Software, formal analysis, validation, investigation, visualization, methodology, writing–original draft. **Y. Chen:** Resources, data curation, project administration. **D. Ai:** Resources, data curation, project administration. **Z. Zhu:** Resources. **W. Zhao:** Resources. **M. Fan:** Resources. **L. Li:** Resources. **H. Zhu:** Funding acquisition. **F. Li:** Resources. **Y. Xu:** Resources. **L. Yu:** Resources. **Z. Wang:** Software, formal analysis. **J. Wang:** Visualization. **Q. Liu:** Resources. **J. Deng:** Resources. **S. Hao:** Resources. **Q. Fan:** Resources. **J. Ye:** Resources. **J. Zhou:** Resources. **C. Wu:** Resources. **H. Tang:** Resources. **Q. Lin:** Resources. **J. Li:** Resources. **Y. Li:** Resources. **S. Wei:** Resources. **H. Luo:** Resources. **J. Cao:** Resources. **X. Zheng:** Resources. **G. Huang:** Resources. **Y. Zheng:** Resources, visualization. **B. Ping:** Resources. **K. Zhao:** Conceptualization, resources, data curation, supervision, funding acquisition, project administration, writing–review and editing.

Acknowledgments

The authors would particularly like to acknowledge Prof. Qi Chen (College of Life Sciences, Fujian Normal University, Fuzhou, China) as well as Prof. Harun Badakhshi (Department of Radiation Oncology, Charité School of Medicine and Centre for Cancer Medicine, Berlin, Germany) for their helpful suggestions on this topic.

Note

Supplementary data for this article are available at Clinical Cancer Research Online (http://clincancerres.aacrjournals.org/).

Received December 9, 2024; revised January 21, 2025; accepted March 4, 2025; posted first March 7, 2025.

References

1. Herrera FG, Bourhis J, Coukos G. Radiotherapy combination opportunities leveraging immunity for the next oncology practice. CA Cancer J Clin 2017;67:65–85.
2. Stone HB, Peters LJ, Milas L. Effect of host immune capability on radiocurability and subsequent transplantability of a murine fibrosarcoma. J Natl Cancer Inst 1979;63:1229–35.
3. Kim R, Emi M, Tanabe K, Arihiro K. Immunobiology of the sentinel lymph node and its potential role for antitumour immunity. Lancet Oncol 2006;7:1006–16.
4. Takeshima T, Chamoto K, Wakita D, Ohkuri T, Togashi Y, Shirato H, et al. Local radiation therapy inhibits tumor growth through the generation of tumor-specific CTL: its potentiation by combination with Th1 cell therapy. Cancer Res 2010;70:2697–706.
5. Buchwald ZS, Nasti TH, Lee J, Eberhardt CS, Wieland A, Im SJ, et al. Tumor-draining lymph node is important for a robust abscopal effect stimulated by radiotherapy. J Immunother Cancer 2020;8:e000867.
6. Murphy KM, Weaver C. Janeway's Immunobiology. 9th Edition. Garland Science; 2016. p. 924.
7. Van Meerhaeghe T, Néel A, Brouard S, Degauque N. Regulation of CD8 T cell by B-cells: a narrative review. Front Immunol 2023;14:1125605.
8. Cui C, Wang J, Fagerberg E, Chen P-M, Connolly KA, Damo M, et al. Neoantigen-driven B cell and CD4 T follicular helper cell collaboration promotes anti-tumor CD8 T cell responses. Cell 2021;184:6101–18.e13.
9. Darragh LB, Gadwa J, Pham TT, Van Court B, Neupert B, Olimpo NA, et al. Elective nodal irradiation mitigates local and systemic immunity generated by combination radiation and immunotherapy in head and neck tumors. Nat Commun 2022;13:7015–33.
10. Marciscano AE, Ghasemzadeh A, Nirschl TR, Theodros D, Kochel CM, Francica BJ, et al. Elective nodal irradiation attenuates the combinatorial efficacy of stereotactic radiation therapy and immunotherapy. Clin Cancer Res 2018;24:5058–71.
11. Liu Z, Yu Z, Chen D, Verma V, Yuan C, Wang M, et al. Pivotal roles of tumor-draining lymph nodes in the abscopal effects from combined immunotherapy and radiotherapy. Cancer Commun (Lond) 2022;42:971–86.
12. Bradley JD, Sugawara S, Lee KHH, Ostoros G, Demirkazik A, Zemanova V, et al. Durvalumab in combination with chemoradiotherapy for patients with unresectable stage III NSCLC: final results from PACIFIC-2. ESMO Open 2024;9:102986.
13. Liu X, Zhang Y, Yang KY, Zhang N, Jin F, Zou G-R, et al. Induction-concurrent chemoradiotherapy with or without sintilimab in patients with locoregionally advanced nasopharyngeal carcinoma in China (CONTINUUM): a multicentre, open-label, parallel-group, randomised, controlled, phase 3 trial. Lancet 2024;403:2720–31.
14. Tao Y, Biau J, Sun XS, Sire C, Martin L, Alfonsi M, et al. Pembrolizumab versus cetuximab concurrent with radiotherapy in patients with locally advanced squamous cell carcinoma of head and neck unfit for cisplatin (GORTEC 2015-01 PembroRad): a multicenter, randomized, phase II trial. Ann Oncol 2023;34:101–10.
15. Lee NY, Ferris RL, Psyrri A, Haddad RI, Tahara M, Bourhis J, et al. Avelumab plus standard-of-care chemoradiotherapy versus chemoradiotherapy alone in patients with locally advanced squamous cell carcinoma of the head and neck: a randomised, double-blind, placebo-controlled, multicentre, phase 3 trial. Lancet Oncol 2021;22:450–62.
16. Lorusso D, Xiang Y, Hasegawa K, Scambia G, Leiva M, Ramos-Elias P, et al. Pembrolizumab or placebo with chemoradiotherapy followed by pembrolizumab or placebo for newly diagnosed, high-risk, locally advanced cervical cancer (ENGOT-cx11/GOG-3047/KEYNOTE-A18): overall survival results from a randomised, double-blind, placebo-controlled, phase 3 trial. Lancet 2024;404:1321–32.
17. Chen Y, Ye J, Zhu Z, Zhao W, Zhou J, Wu C, et al. Comparing paclitaxel plus fluorouracil versus cisplatin plus fluorouracil in chemoradiotherapy for locally advanced esophageal squamous cell cancer: a randomized, multicenter, phase III clinical trial. J Clin Oncol 2019;37:1695–703.
18. Ai D, Ye J, Wei S, Li Y, Luo H, Cao J, et al. Comparison of 3 paclitaxel-based chemoradiotherapy regimens for patients with locally advanced esophageal squamous cell cancer: a randomized clinical trial. JAMA Netw Open 2022;5:e220120.
19. Martinez-Monge R, Fernandes PS, Gupta N, Gahbauer R. Cross-sectional nodal atlas: a tool for the definition of clinical target volumes in three-dimensional radiation therapy planning. Radiology 1999;211:815–28.
20. Jin J-Y, Hu C, Xiao Y, Zhang H, Paulus R, Ellsworth SG, et al. Higher radiation dose to the immune cells correlates with worse tumor control and overall survival in patients with stage III NSCLC: a secondary analysis of RTOG0617. Cancers (Basel) 2021;13:6193.
21. Vesprini D, Sia M, Lockwood G, Moseley D, Rosewall T, Bayley A, et al. Role of principal component analysis in predicting toxicity in prostate cancer patients treated with hypofractionated intensity-modulated radiation therapy. Int J Radiat Oncol Biol Phys 2011;81:e415-21.
22. Légal J-D, De Crevoisier R, Lartigau E, Morsli K, Dossou J, Chavaudra N, et al. Chromosomal aberrations induced by chemotherapy and radiotherapy in lymphocytes from patients with breast carcinoma. Int J Radiat Oncol Biol Phys 2002;52:1186–95.
23. d'Alesio V, Pacelli R, Durante M, Canale Cama G, Cella L, Gialanella G, et al. Lymph nodes in the irradiated field influence the yield of radiation-induced chromosomal aberrations in lymphocytes from breast cancer patients. Int J Radiat Oncol Biol Phys 2003;57:732–8.

24. Ganusov VV, Auerbach J. Mathematical modeling reveals kinetics of lymphocyte recirculation in the whole organism. PLoS Comput Biol 2014;10:e1003586.
25. Fang P, Shiraishi Y, Verma V, Jiang W, Song J, Hobbs BP, et al. Lymphocyte-sparing effect of proton therapy in patients with esophageal cancer treated with definitive chemoradiation. Int J Part Ther 2018:4:23–32.
26. Lv J, Wei Y, Yin J-H, Chen Y-P, Zhou G-Q, Wei C, et al. The tumor immune microenvironment of nasopharyngeal carcinoma after gemcitabine plus cisplatin treatment. Nat Med 2023;29:1424–36.
27. El Sissy C, Kirilovsky A, Lagorce Pagès C, Marliot F, Custers PA, Dizdarevic E, et al. International validation of the immunoscore biopsy in patients with rectal cancer managed by a watch-and-wait strategy. J Clin Oncol 2024;42:70–80.
28. Nakamura N, Kusunoki Y, Akiyama M. Radiosensitivity of CD4 or CD8 positive human T-lymphocytes by an in vitro colony formation assay. Radiat Res 1990;123:224–7.
29. Ludmir EB, Sherry AD Fellman BM, Liu S, Bathala T, Haymaker C, et al. Addition of metastasis-directed therapy to systemic therapy for oligometastatic pancreatic ductal adenocarcinoma (EXTEND): a multicenter, randomized phase II trial. J Clin Oncol 2024;42:3795–805.
30. Chen Y, Yu R, Liu Y. Combine radiotherapy and immunotherapy in esophageal squamous cell carcinoma. Crit Rev Oncol Hematol 2023;190:104115.
31. Huang Q, Wu X, Wang Z, Chen X, Wang L, Lu Y, et al. The primordial differentiation of tumor-specific memory $CD8^+$ T cells as bona fide responders to PD-1/PD-L1 blockade in draining lymph nodes. Cell 2022;185:4049–66.e25.
32. Rahim MK, Okholm TLH, Jones KB, McCarthy EE, Liu CC, Yee JL, et al. Dynamic $CD8^+$ T cell responses to cancer immunotherapy in human regional lymph nodes are disrupted in metastatic lymph nodes. Cell 2023;186:1127–43.e18.
33. Chang JY, Lin SH, Dong W, Liao Z, Gandhi SJ, Gay CM, et al. Stereotactic ablative radiotherapy with or without immunotherapy for early-stage or isolated lung parenchymal recurrent node-negative non-small-cell lung cancer: an open-label, randomised, phase 2 trial. Lancet 2023;402:871–81.